TRANSIENT GROWTH MECHANISMS OF RESISTIVE DRIFT-WAVES

Suzana J. Camargo[1], Michael K. Tippett[2], and Iberê L. Caldas[3]

[1]*Universidade Estadual Paulista, Campus de Guaratinguetá, Brazil*
[2]*Centro de Previsão do Tempo e Estudos Climáticos, INPE, SP, Brazil*
[3]*Instituto de Física, Universidade de São Paulo, São Paulo, SP, Brazil*

1. Introduction

Normal mode analysis has been applied to many fluid dynamic stability problems with great success. However, there are some notable cases where the predictions of normal mode analysis fail to correspond to observed phenomena. In particular, normal mode analysis predicts a transition to turbulence for some flows at a much higher Reynolds numbers than that seen in experiment. Recent studies have shown that for some problems, normal mode analysis only gives a partial description of the properties of the linear perturbation equation [1, 2]. When the eigenmodes of the linear system are not orthogonal and complete, or equivalently when the system is *nonnormal*, general solutions of the system may present behavior quite different from that suggested by normal mode analysis [3]. Drift-wave turbulence is considered to be a possible cause of anomalous transport in the cool plasma edge region of tokamaks. Here, nonnormal analysis methods are used to study the linear properties of the Hasegawa-Wakatani drift-wave turbulence model [4].

2. Model

Neglecting the nonlinear terms of the Hasegawa-Wakatani equations and expanding the potential and density in a double Fourier series in the nondimensionalized slab variables x and y gives the system

$$\frac{d}{dt}\mathbf{u_k} = \mathbf{A_k}\mathbf{u_k}\,, \tag{1}$$

for the time evolution of the Fourier components of ϕ and n, where $\mathbf{k} = (k_x, k_y)$ and

$$\mathbf{u_k} = \begin{pmatrix}\phi_\mathbf{k}\\ n_\mathbf{k}\end{pmatrix}\,, \quad \mathbf{A_k} = \begin{pmatrix}-\mathcal{C}/k^2 - \nu_\phi k^4 & \mathcal{C}/k^2\\ -ik_y + \mathcal{C} & -\mathcal{C} - \nu_n k^4\end{pmatrix}\,, \quad k = \sqrt{k_x^2 + k_y^2}\,; \tag{2}$$

ν is a small numerical diffusion coefficient as in [5]. The adiabaticity parameter $\mathcal{C}$, which determines the character of the system is defined as [5]

$$\mathcal{C} = \frac{T}{n_0 e^2 \eta_\parallel}\frac{k_\parallel^2}{c_s/L_n}\,. \tag{3}$$

For $\mathcal{C} \gg 1$, the system is almost normal and its behavior is modal. In the nondissipative limit, $\mathcal{C} = 0$, there is nonmodal algebraic growth of the density as was observed in nonlinear simulations of the tri-dimensional Hasegawa-Wakatani system [6].

We use as diagnostics the energy growth ratio $\xi(t) = \|\mathbf{u}(t)\|/\|\mathbf{u}(0)\|$, and its growth rate $\beta(t) = t^{-1} \ln \xi(t)$. The notation $\xi_0(t)$ indicates that $\mathbf{u}(0)$ is chosen to excite the fastest growing modal instablity. The notation $\xi_1(t)$ indicates that $\mathbf{u}(0)$ is chosen such that $\xi(t)$ is maximized. The quantity $\xi_1(t)$ is related to $\mathbf{A}$ by $\xi_1(t) = \| \exp \mathbf{A}t\|$ and is the largest factor by which the initial fluctuation energy can be amplified. The ensemble-averaged energy growth and phase shift of random initial conditions can also be calculated [7].

3. Results

Assuming exponential time-dependence flucuations, e.g., $\sim e^{zt}$, reduces Eq. (1) to the eigenvalue problem $(z\mathbf{I} - \mathbf{A})\,\mathbf{u} = 0$. In Figs. 1(a) and (b), we plot in the complex z-plane the spectra $\Lambda(\mathbf{A})$ (in black) of $\mathbf{A}$, for $\mathcal{C} = 10^{-5}$ and $\mathcal{C} = 10^{-3}$. The modal growth rate is $\beta_0 = \max \mathrm{Re}\, \Lambda(\mathbf{A})$. Transient growth properties are related to the *pseudospectrum* of $\mathbf{A}$ obtained by the approximate solution of the eigenvalue problem. The complex number z is in the ϵ-pseudospectrum $\Lambda_\epsilon(\mathbf{A})$ if $z \in \Lambda(\mathbf{A} + \mathbf{E})$ for $\|\mathbf{E}\| \leq \epsilon$. Monte Carlo estimates of the pseudospectrum (in gray) in Figs. 1(a) and (b) show that for small values of $\mathcal{C}$ the eigenvalues of $\mathbf{A}$ are highly sensitive to perturbations. The extension $\alpha(\epsilon)$ of the pseudospectrum into the right half-plane is defined by

$$\alpha(\epsilon) = \max_{z \in \Lambda_\epsilon(\mathbf{A})} \mathrm{Re}\, z\,. \tag{4}$$

The maximum growth is modal, $\xi_1(t) = e^{\beta_0 t}$, if and only if for all $\epsilon > 0$, $\alpha(\epsilon) - \alpha(0) \leq \epsilon$, that is to say, if a perturbation of size ϵ to $\mathbf{A}$ moves its eigenvalues by at most a distance ϵ further into the real half-plane. A lower bound on nonmodal growth is

$$\max_{t \geq 0} \xi_1(t) = \max_{t \geq 0} \|e^{\mathbf{A}t}\| \geq \max_{\epsilon > 0} \frac{\alpha(\epsilon) - \alpha(0)}{\epsilon} e^{\beta_0 t}\,. \tag{5}$$

A Monte Carlo estimate of $(\alpha(\epsilon) - \alpha(0))/\epsilon$ in Fig. 1(c) shows that for $\mathcal{C} = 10^{-3}$ and $\mathcal{C} = 10^{-5}$ transient nonmodal growth is enhanced by at least a factor of 6.8 and 45 respectively compared to modal growth. For $\mathcal{C} = 1$, $(\alpha(\epsilon) - \alpha(0))/\epsilon \approx 1$; the pseudospectrum does not predict enhanced nonmocal energy growth. The dependence on ϵ indicates that the enhanced nonmodal growth occurs at different wavenumbers than those of the fastest growing modal instability.

Calculations of the finite-time growth rate $\beta_1(t)$ and the modal growth rate β_0 in Fig. 2 indicate that the finite-time growth rates for small $\mathcal{C}$ and $t = 10$ are slightly larger than those for $\mathcal{C} = 0.1$. This dependence on $\mathcal{C}$ is the opposite of that seen in the modal growth rate which peaks for $\mathcal{C} \sim 0.1$ and decreases both sides. Examination of $\beta_1(t)$ as a function of k_y indicates that the nonmodal growth for small $\mathcal{C}$ is a broad-spectrum phenomena [7]. As the time t increases, the limit $\beta_1(t) \to \beta_0$ must hold. Figure 2(a) shows that for large values of $\mathcal{C}$ β_0 and β_1 coincide for all values of t. For small enough $\mathcal{C}$, $\beta_1(t)$ does not depend on $\mathcal{C}$ and the

$\mathcal{C} = 0$ result of pure algebraic growth $\sim k_y t$ is recovered. Denoting by k_0^{max} and $k_1^{max}(t)$ the perpendicular wave number corresponding to the growth rates β_0 and $\beta_1(t)$, Fig. 2(b) indicates that at a particular time t, the maximum growth wavenumber is the same as the maximum modal growth wavenumber, $k_1^{max}(t) \approx k_0^{max}$ for values of the adiabatic parameter $\mathcal{C}$ above some cut-off $\mathcal{C}_{crit}(t)$ and for $\mathcal{C} < \mathcal{C}_{crit}(t)$, the maximum growth wavenumber is the same as the short-time maximum energy growth wavenumber; the cut-off value $\mathcal{C}_{crit}(t)$ is a decreasing function of time.

A stochastic forcing plus a damping term are added to the linear equation following [8]. The energy spectrum of the statistically steady-state obtained is compared with that of an equivalent normal system, i.e., one with the same eigenvalues. Fig. 3 indicates that nonmodal effects lead to anisotropy in the energy spectrum and saturation levels quite different from those predicted by the modal properties of the system.

4. Conclusions

The main points of this work are: The pseudospectrum of the Hasegawa-Wakatani system shows that for small $\mathcal{C}$, nonmodal growth is larger than the modal growth and occurs at different wavenumbers. For $\mathcal{C} \ll 1$, drift-waves with $\beta_0 \approx 0$ have nonmodal growth rates comparable to the modal growth rates of the most unstable drift-waves ($\mathcal{C} = 0.1$). The nonmodal behavior is generally a broad-spectrum phenomena.

Nonlinear simulations of the Hasegawa-Wakatani system found that the saturation time decreased and the saturation level increased for small $\mathcal{C}$ in contrast to modal growth rate [5]. This behavior is consistent with the nonmodal linear mechanisms seen here. Further studies of the stochastically forced system with different types of forcing are being developed in order to model better the nonlinear simulations.

Acknowledgement

This work was supported by CNPq (Grant 381737/97-73) and by FAPESP (Grant 96/5388-0).

References

[1] L.N. Trefethen, A.E. Trefethen, and S.C. Reddy: Science **261**, 578 (1993).
[2] B.F. Farrell and P. Ioannou: J. Atmos. Sci. **53**, 2025 (1996).
[3] K.M. Butler and B.F. Farrell: Phys. Fluids A **4**, 1637 (1992).
[4] A. Hasegawa and M. Wakatani: Phys. Rev. Lett. **50**, 682 (1985).
[5] S.J. Camargo, D. Biskamp, and B.D. Scott: Phys. Plasmas **2**, 48 (1995).
[6] D. Biskamp and A. Zeiler: Phys. Rev. Lett. **74**, 706 (1995).
[7] S.J. Camargo, M.K. Tippett, and I. Caldas: Technical Report P-1296, Instituto de Física da Universidade de São Paulo, *to appear in* Phys. Rev. E, August (1998).
[8] B.F. Farrell and P.J. Iannou: Phys. Fluids A **5**, 2600 (1993).

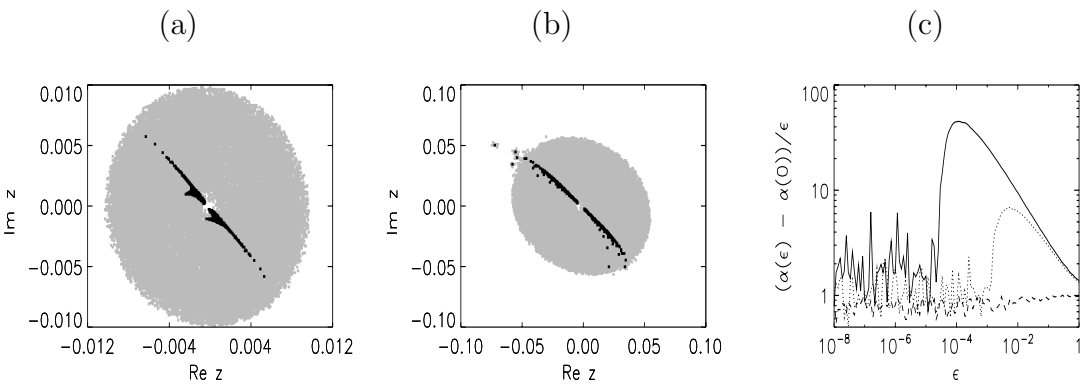

Figure 1. The spectrum $\Lambda(\mathbf{A})$ (black) and ϵ-pseudospectrum $\Lambda_\epsilon(\mathbf{A})$ (gray) plotted in the complex z-plane for (a) $\mathcal{C} = 10^{-5}$ and $\epsilon = 10^{-4}$ (b) $\mathcal{C} = 10^{-3}$ and $\epsilon = 3.2 \times 10^{-3}$. Panel (c) The quantity $(\alpha(\epsilon) - \alpha(0))/\epsilon$ plotted as a function of ϵ for $\mathcal{C} = 10^{-5}$ (solid-line), $\mathcal{C} = 10^{-3}$ (dotted-line) and $\mathcal{C} = 1$ (dashed line).

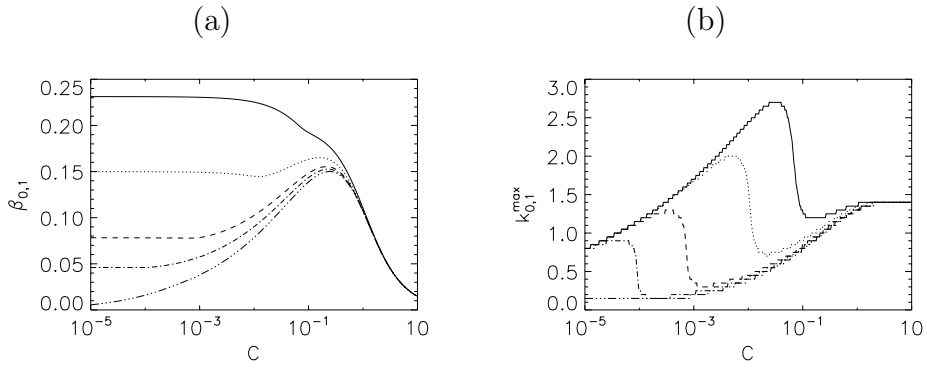

Figure 2. (a) The growth rates β_0 (dot-dot-dot-dash) and $\beta_1(t)$ for $t = 10$ (solid), $t = 20$ (dotted), $t = 50$ (dashed) and $t = 100$ (dot-dash) plotted as functions of $\mathcal{C}$. (b) Values of k_0^{max} and $k_1^{max}(t)$ for the same values of t (and line styles) plotted as a function of $\mathcal{C}$.

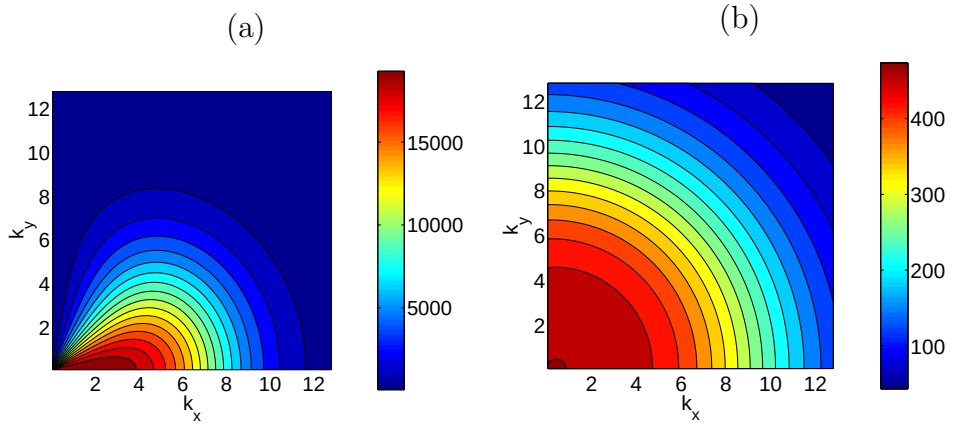

Figure 3. Bidimensional energy spectrum obtained from the stochastically forced linear system (a) and the equivalent normal system (b) obtained for $\mathcal{C} = 10^{-5}$ and $\nu = 10^{-5}$.